SENSORES REMOTOS PARA DETECCIÓN Y MONITOREO DE ENFERMEDADES

Dr. Mauricio Serrano

AF-109

28/setiembre/2024

Por qué evaluar enfermedades de plantas con herramientas tecnológicas?

- Próximamente discutiremos la importancia de cuantificar enfermedades
  - *"La piedra angular del análisis de una epidemia"*
  - *Buscamos exactitud, presición, repetibilidad.*
  - *Dependemos de estimaciones visuales*
    - *Se requieren evaluadores entrenados.*
  - *También podemos usar análisis de imágenes para determinar el valor real de intensidad de la enfermedad*

- Entonces, por qué no usar herramientas similares para detectar y cuantificar enfermedades en cultivos?
  - *Exactitud, presición*
  - *Muestreo no invasivo*
  - *Conveniencia, Costo?*
  - *Potencial aplicación a gran escala en agricultura de presición.*

Sensing

Detection

Yellow rust

Powdery mildew

Brown rust

Application plan
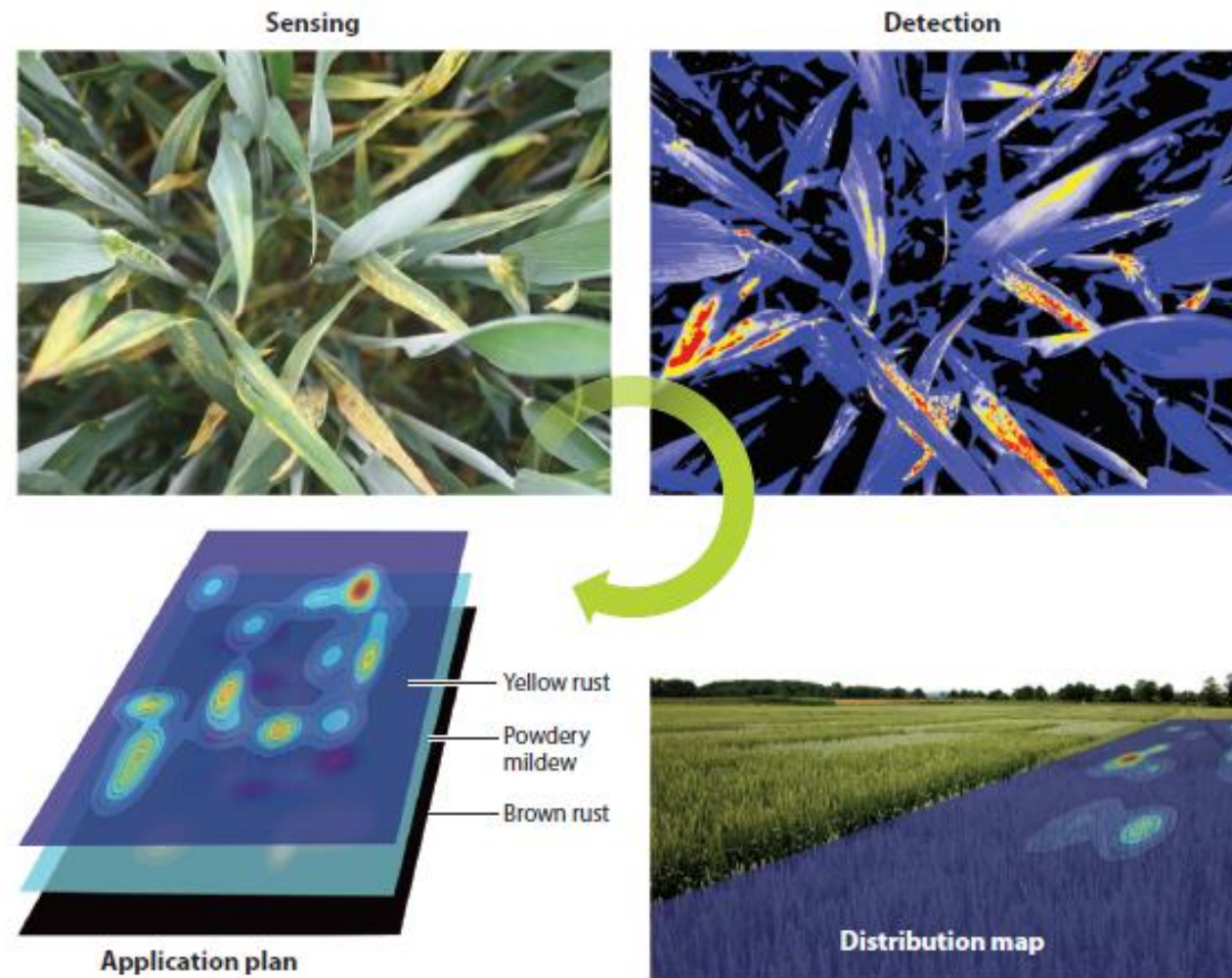
Distribution map

Figure 4

Potential analysis pipeline from sensing plant canopies to a site-specific fungicide application. In a first step, the canopy is assessed with a hyperspectral imaging camera in nadir. Secondly, an algorithm calculates the disease severity within the image. Thirdly, the disease severity is linked to the geographic distribution within the field by a distribution map, and finally, application plans can be determined based on the combined distribution maps of multiple diseases.

Malheim et al 2018

Uso de sensores remotos

- **Remote sensing:** "medición o adquisición de información de alguna propiedad de un objeto o fenómeno mediante un dispositivo que no está en contacto cercano" (Campbell y Madden, 1990).
  - *Se refiere principalmente a dispositivos para medir radiación reflejada y la captura de datos o fotografías*

- **El principio:** Una planta con estrés presenta un patrón de absorción/reflexión diferente al de una planta sana.
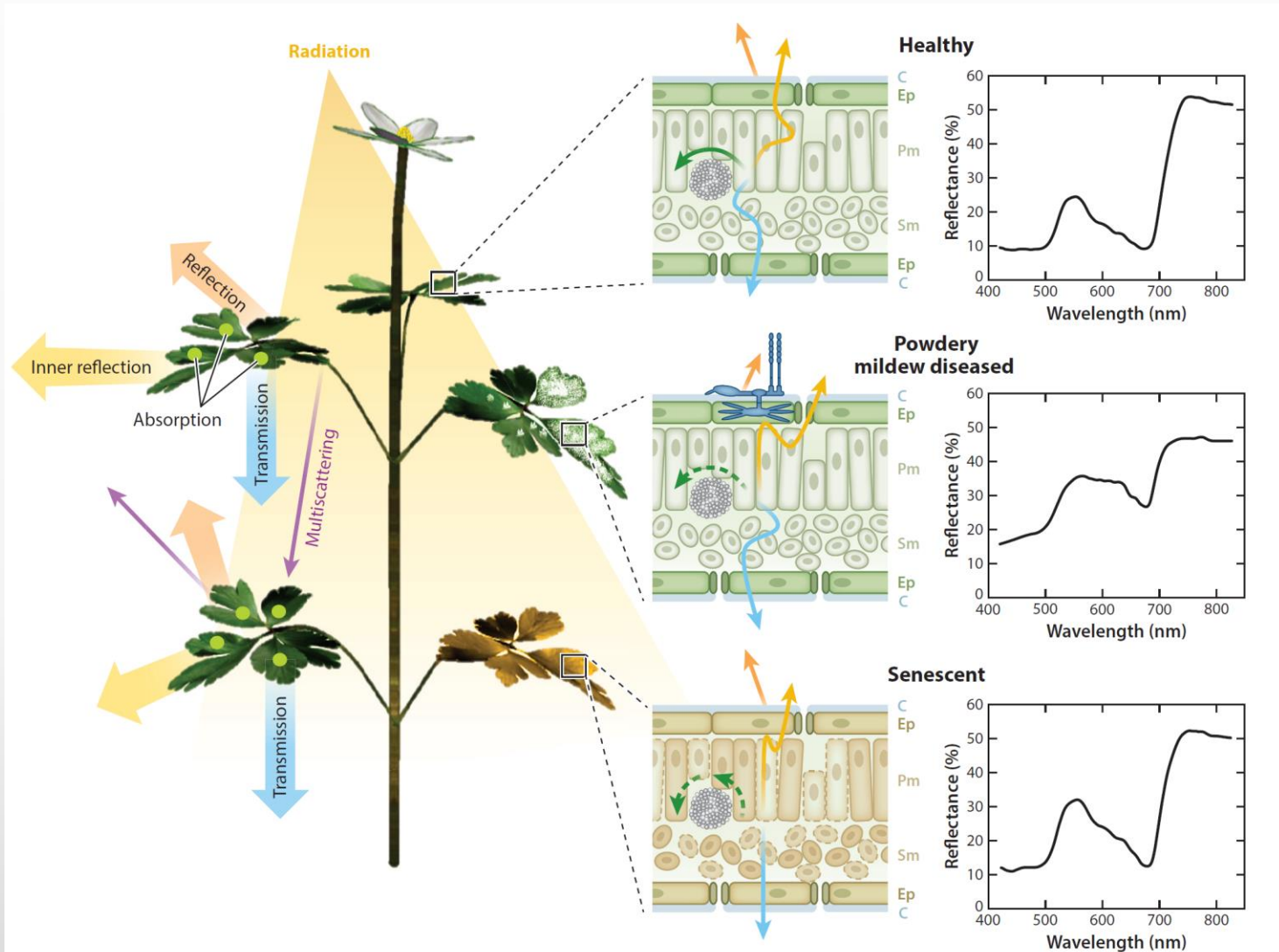
El espectro electromagnético

https://en.wikipedia.org/wiki/Electromagnetic_spectrum
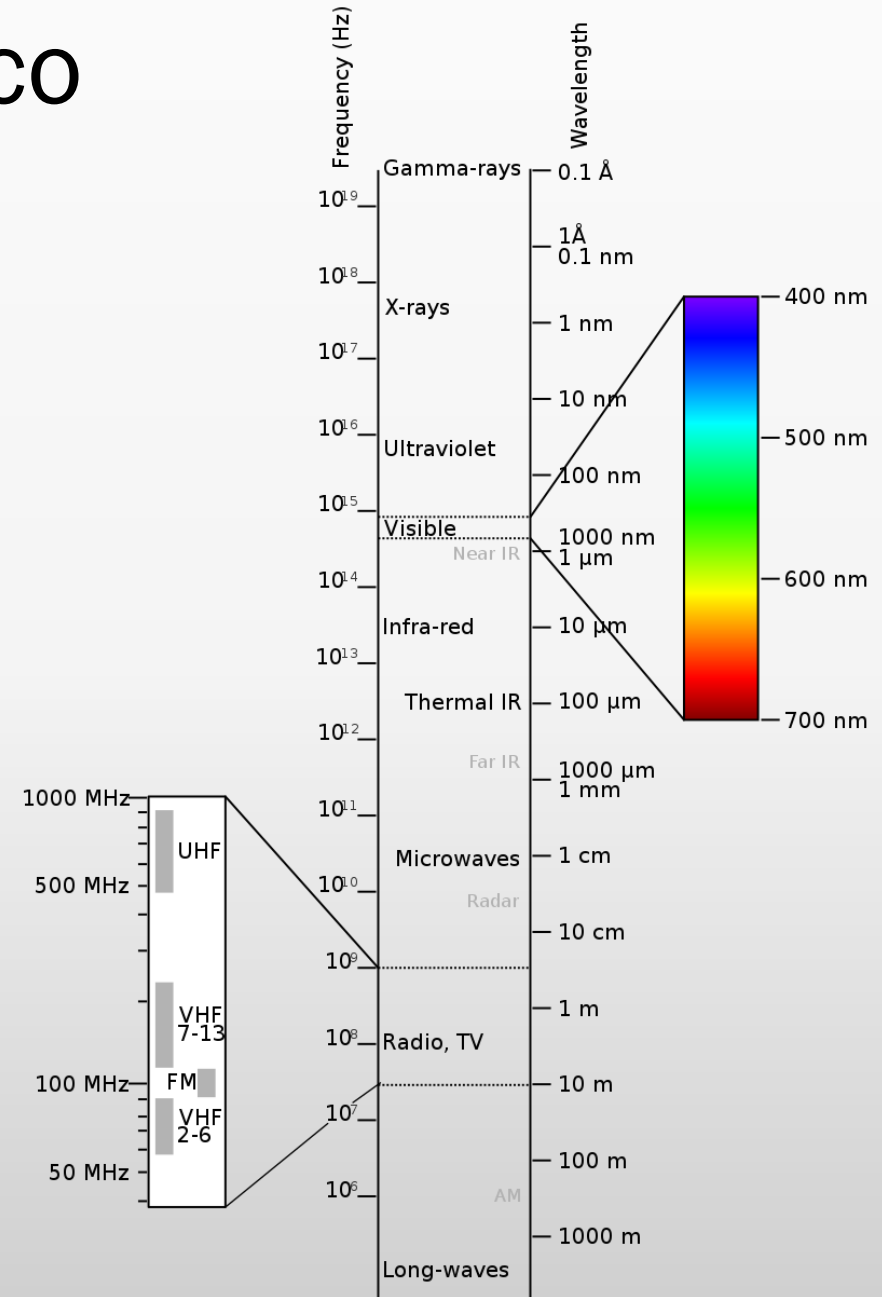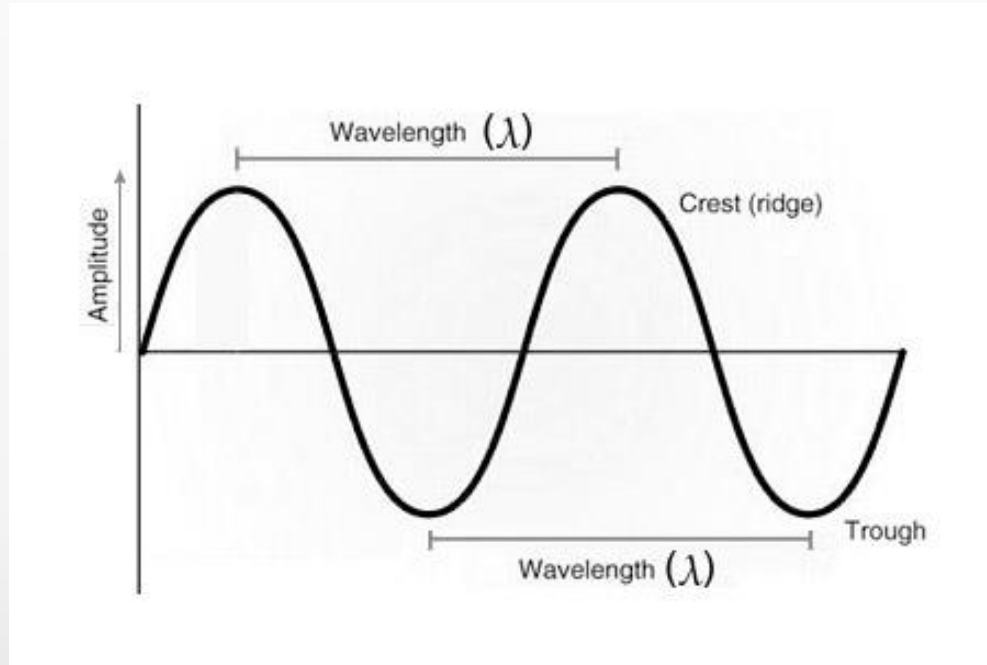
Figure 1

Interaction of plant tissue with incoming radiation depends on structural and chemical leaf properties. (*Left*) Light from the sun or an artificial light source can be transmitted, absorbed, or reflected. (*Middle*) The proportion and intensity of light that is reflected depends on the condition of the leaf. (*Right*) Characteristic spectral reflectance signatures can be assigned to the health status or disease infestation of plant tissue. Abbreviations: C, cuticula; Ep, epidermis; Pm, palisade mesophyll; Sm, spongy mesophyll.

La radiación electromagnética que emerge de una planta o dosel está determinada por las interacciones (reflexión, transmisión, absorción) entre la radiación incidente y los tejidos de la planta

Malheim et al 2018
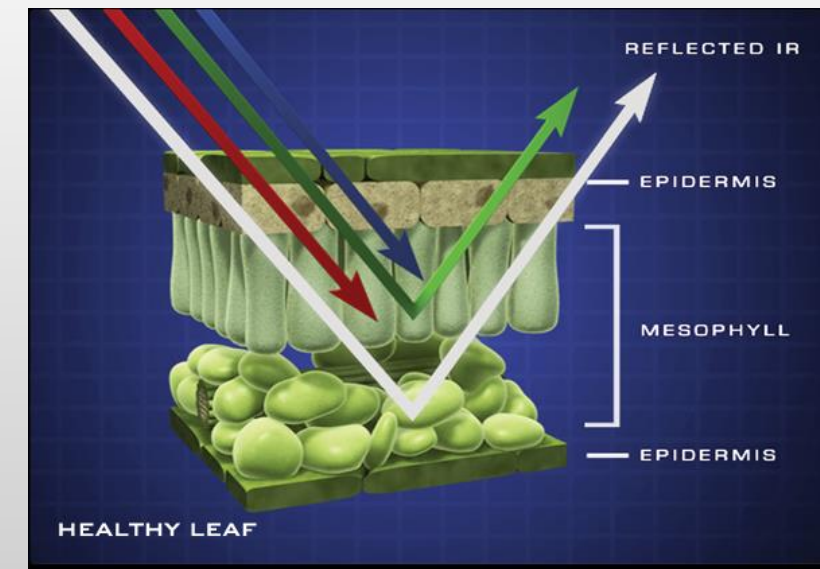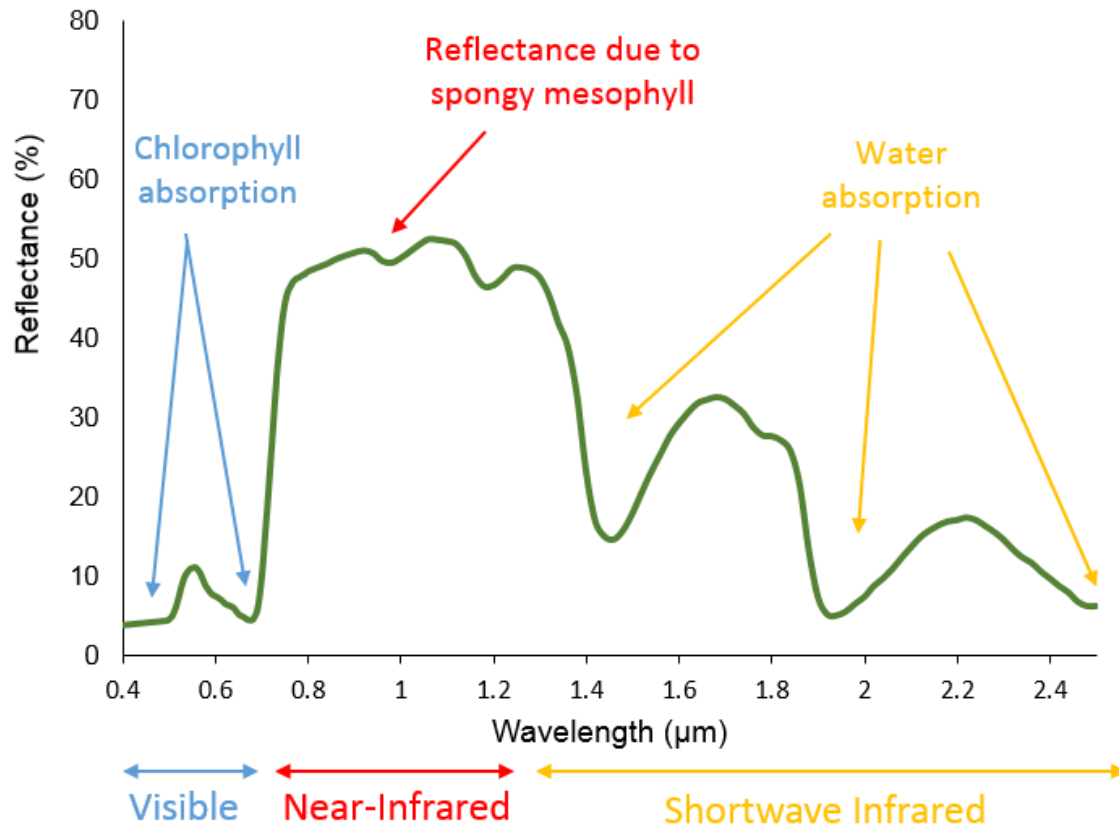
$$Firma\ espectral = \frac{radiación\ reflejada}{radiación\ incidente} * 100$$

La firma espectral de la hoja o dosel se puede obtener para cada longitud de onda del espectro.

Los cambios en esta firma (reflectancia) pueden usarse como un método indirecto para detectar o cuantificar enfermedades en la planta.
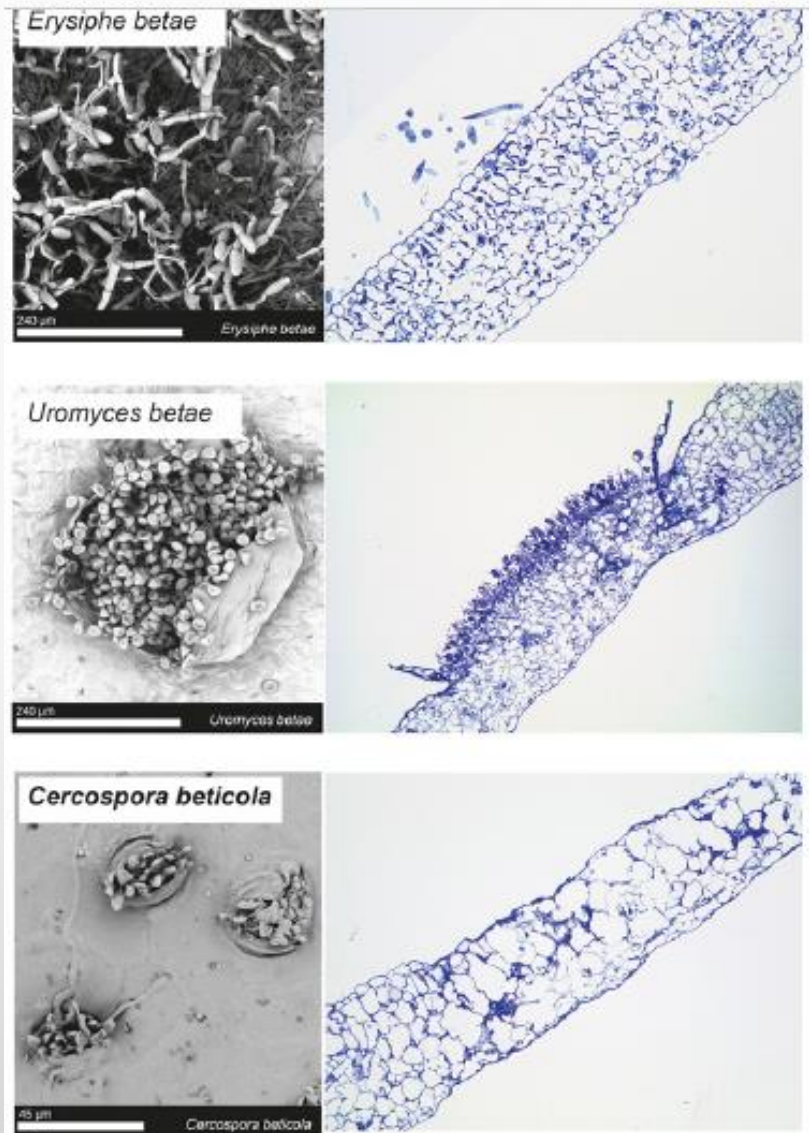
Fig. 4. Detailed view of the host-pathogen interaction can be obtained by electron microscopy or semithin sections from light microscopy. This indicated the highly specific appearance and influence of different foliar diseases in the example of sugar beet leaf diseases.

Fig. 5. Characteristic spectral signatures of barley leaves diseased with net blotch, rust, and powdery mildew, respectively.

Malheim 2015

Fig. 4 Field reflectance spectra for healthy tomatoes plants (*H*) and plants infected with late blight disease increasing severity (from 1 to 4). *S* is the average spectrum for soil. The insert is an enlarged view of the abrupt changes at approximately 1,040 nm (from Zhang et al. 2003) (courtesy of the International Journal of Applied Earth Observation and Geoinformation, edited by Elsevier)
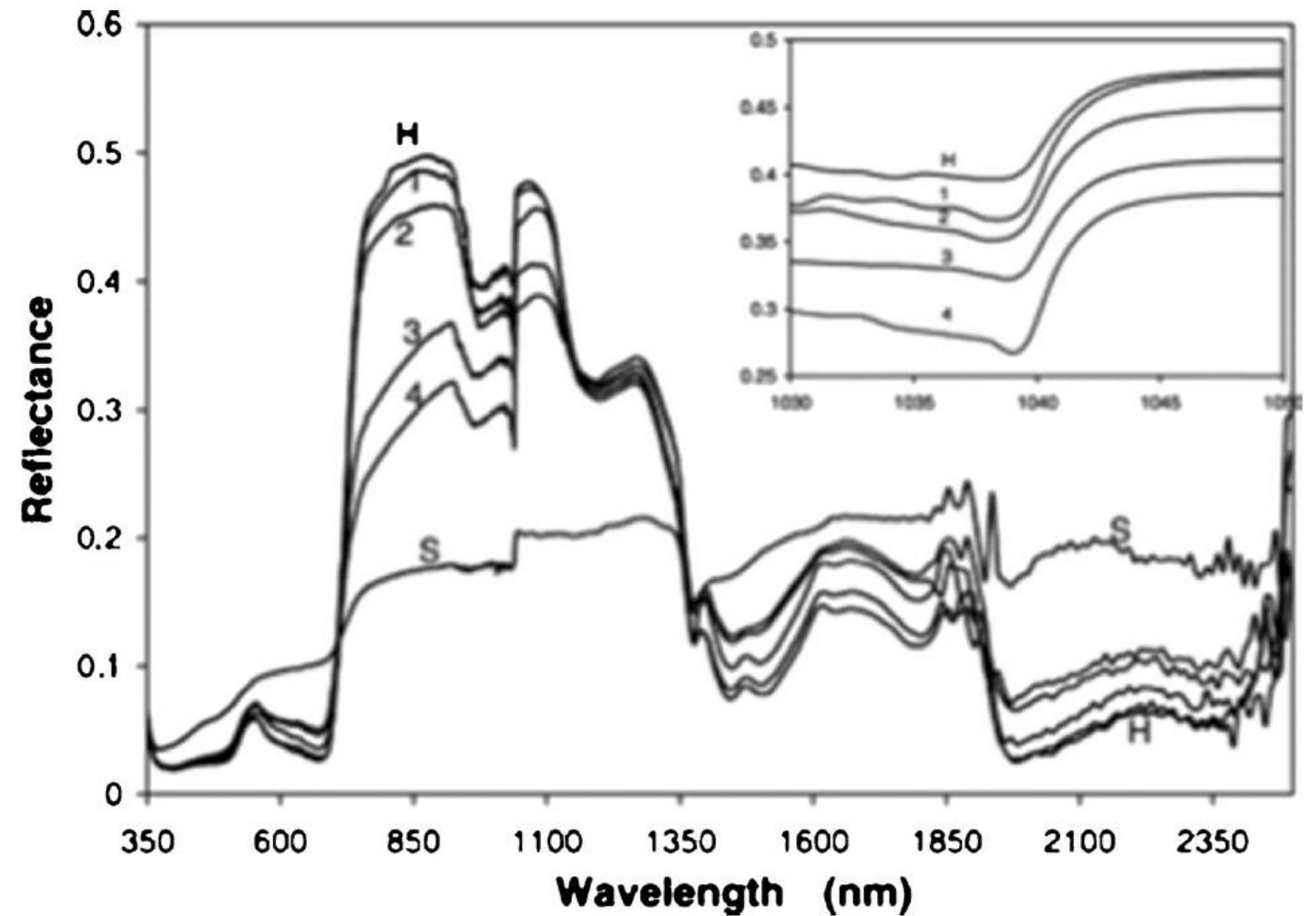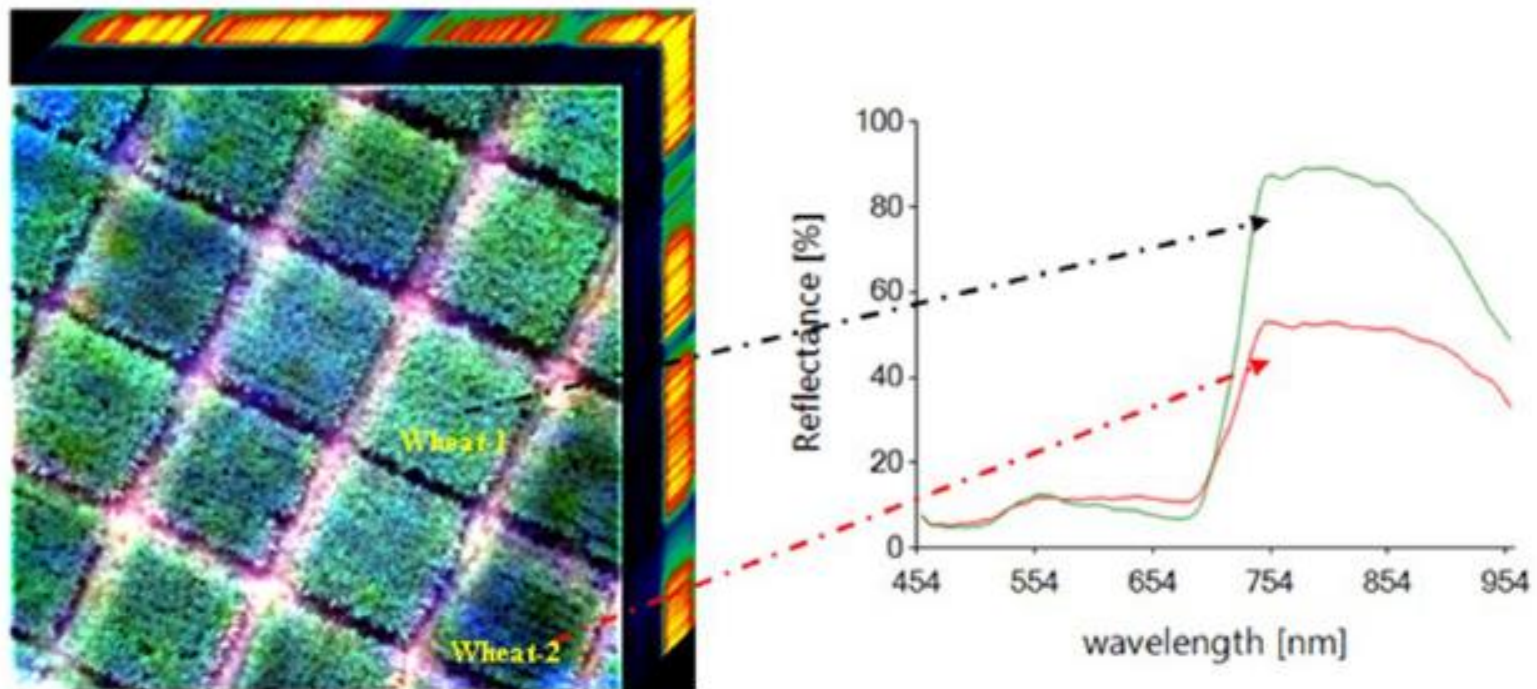
Phytophthora infestans en tomate

Martinelli 2015

FIGURE 6 | The distribution of hyperspectral imaging in wheat breeding.

Yang et al 2017

4 tipos de daños que se pueden ser detectados con sensores remotos

1. Reducción de la biomasa del cultivo y disminución del índice de área foliar

2. Lesiones causadas por la infección del patógeno

3. Destrucción de pigmentos

4. Marchitamiento

Table 1

Plant damages due to diseases and pests detected by remote sensing.

Plant damages	Representative diseases or pests	Symptoms
1. Reduction of biomass, decrease of LAI	Armyworm in maize	
2. Lesions or pustules due to infection	Yellow rust, powdery mildew in wheat	
3. Destruction of pigments systems (chlorophyll, carotenoid, anthocyanin, etc.)	Bacterial blight of rice	
4. Wilting	Aphid in wheat	

Spodoptera frugiperda

Puccinia striiformis f. sp. tritici)

Blumeria graminis f. sp. tritici

Xanthomonas oryzae pv. oryzae

Cualquier tipo de stress provoca una respuesta de la planta, la cual puede ser detectada por sensores remotos
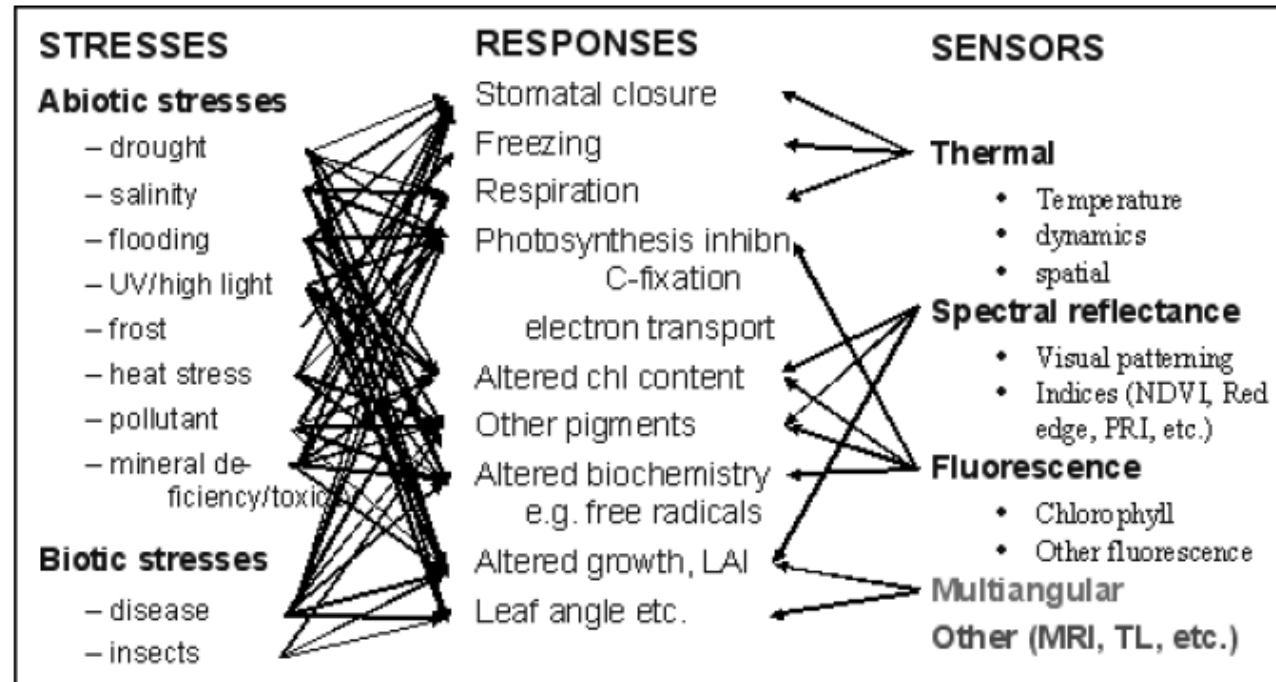

Fig. 1. An illustration of the relationships between primary stresses and the intermediate responses and secondary stresses, together with an indication of which of these intermediate responses are detected by different remote sensing technologies.

Nótese que las respuestas al estrés no son específicas.

Los sensores pueden detectar la respuesta, pero los datos proporcionados son una medición indirecta de lo que podría ser una enfermedad causada por un patógeno o también un estrés abiótico.

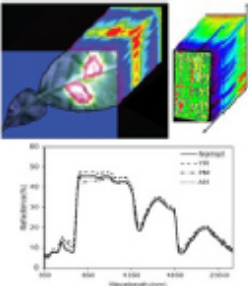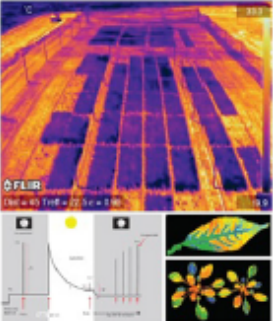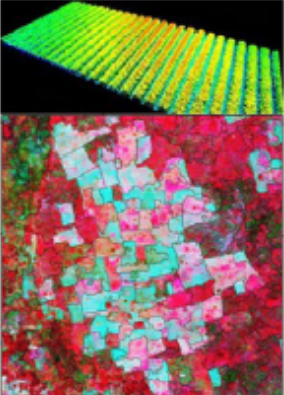# Clasificación de los sistemas de sensores remotos más utilizados

- VIS-SWIR
  - *Visible (400 – 700nm), infrarojo cercano (NIR) (700-1200nm), infrarojo onda corta (SWIR) (1200 – 2400nm)*

- Fluorescent and thermal (100 um)

- SAR (Synthetic Aperture Radar) and Lidar (Light detection and ranging equipment)

Table 2
Remote sensing systems for detection and monitoring plant diseases and pests.

RS systems	Main features	Advantages & Disadvantages	Application maturity	Schematic diagram
VIS-SWIR	Determine damages caused by plant diseases and pests by reflectance in VIS-SWIR region	Stable, offers reliable monitoring results. But performs poorly on early detection	High (Corresponding instruments and algorithms are available at relatively low price)	
Fluorescence & thermal	Capture presymptom physiological changes	Have a potential to provide presymptom detection. But currently difficult to apply in large area	Medium (Most current systems are for research, which are expensive with low applicability)	
SAR & Lidar	Capture structural or morphological changes due to diseases and pests	Able to indicate structural plant changes. The systems and case studies are currently very scarce	Low (Mostly remain at a conceptual stage)	

Notes: the diagrams for demonstration are modified from Box. 2 in Furbank and Tester (2011); Fig. 2, Fig. 3 in Murchie and Lawson (2013).

Uso de sensores VIS-SWIR

Mohsin taking radiometer readings at Hinds farm

Sudden Death Symdrome early symptoms in a farmer's field

Uso de firma espectral para medición de SDS causada por *Fusarium virguliforme* en soya, Ames, Iowa. (Medición de reflectancia a 460, 510 y 710nm)

Late leaf spot of peanut
(Phaeoisariopsis
personata)
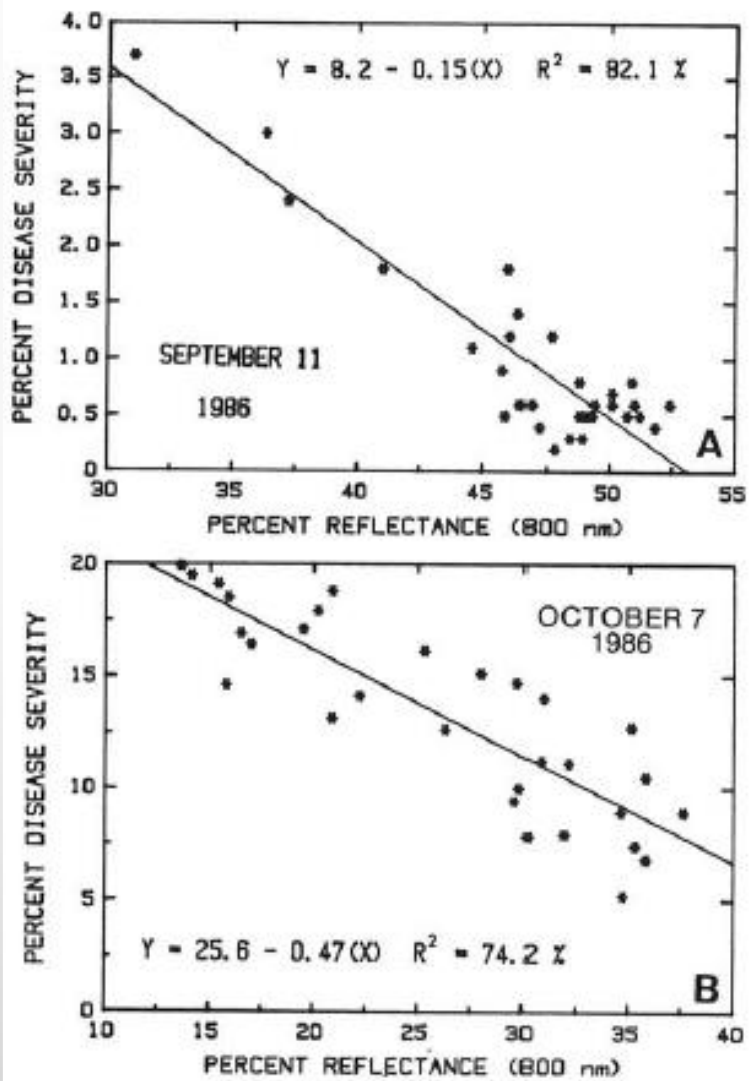
Medición de reflectancia a 800 nm

Nutter et al 1990

Fig. 3. Relationship between visual estimates of percent disease caused by late leaf spot and percent reflectance of sunlight recorded on 11 September (A) and 7 October (B), from peanut canopies treated with different fungicides in 1986 at Plains, GA. Data points are the means of four replications.
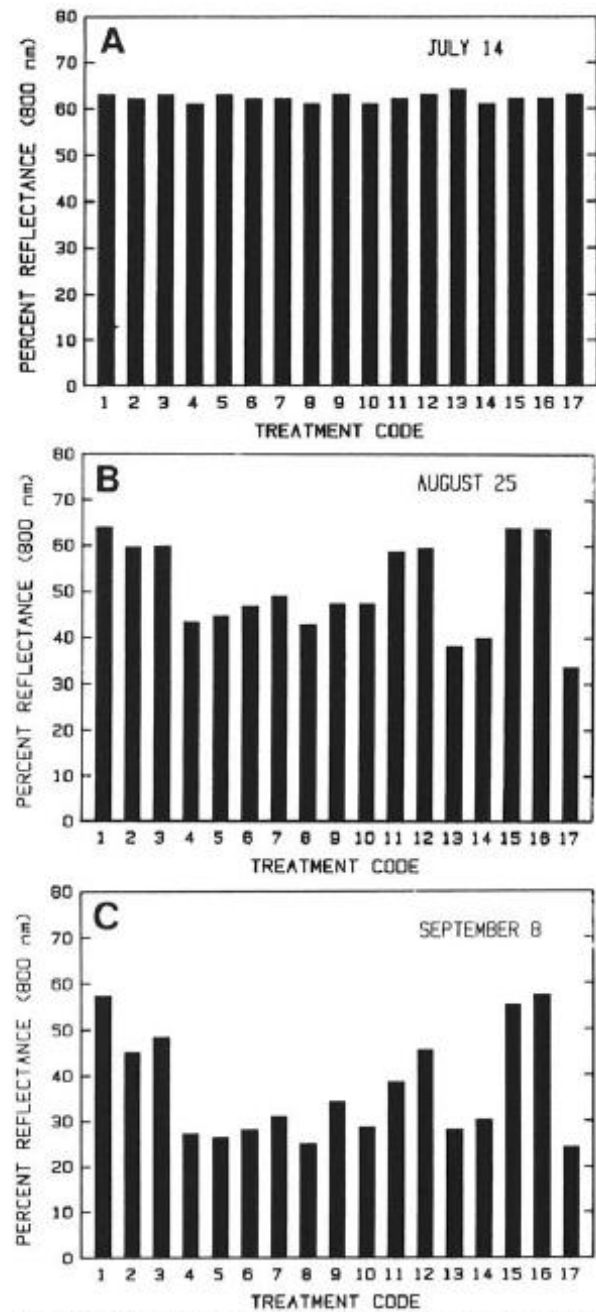
Fig. 2. Percent reflectance of sunlight (800 nm) from peanut canopies treated with different fungicides to control late leaf spot on three dates in 1987. The fungicide code corresponds to the treatment numbers used in Table 4.
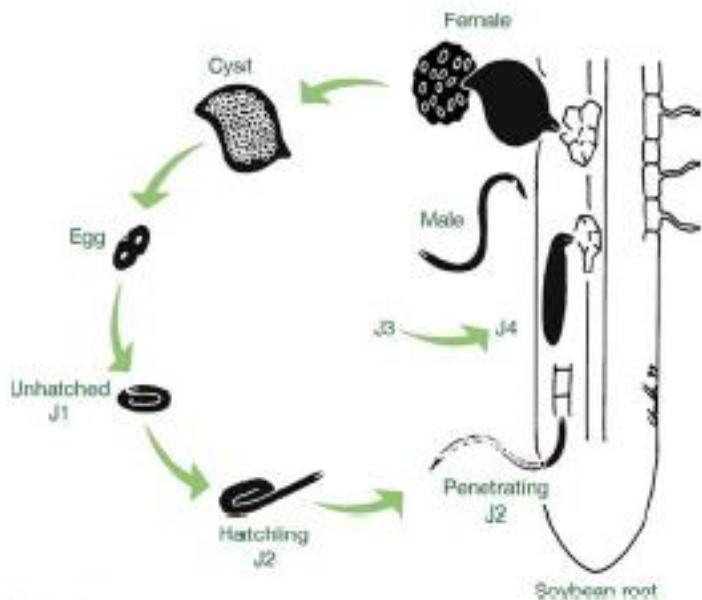
Figure 2

Life cycle of *Heterodera glycines* (all stages not drawn to the same scale) (D.V. Charlson, unpublished). A developed first-stage juvenile (J1) eventually forms in the egg. The J1 molts once within the egg shell, becoming a second-stage juvenile (J2) that hatches from the egg. The J2 penetrates the root and, in a host, develops through the third and fourth juvenile stages (J3 and J4, respectively). Vermiform, adult males fertilize lemon-shaped, adult females and the adult females produce eggs externally, in an egg mass, then fill up internally with eggs.

Niblack et al 2006

Soybean cyst nematode
(Heterodera glycines)

https://cropprotectionnetwork.org/resources/articles/diseases/soybean-cyst-nematode-of-soybean
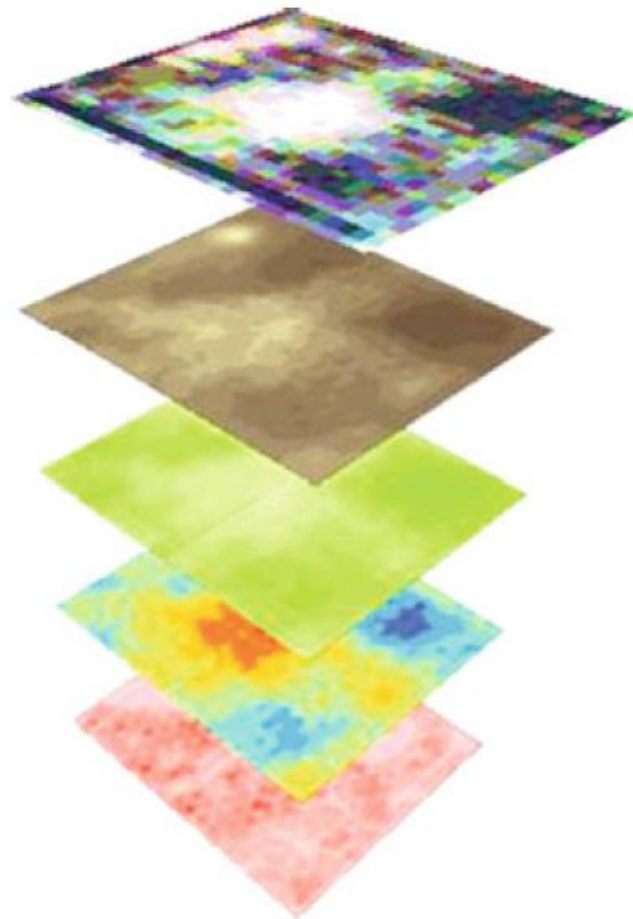
Satellite image (Landsat 7) with 4 m^2 resolution. The darkest colors indicate the healthiest crop areas.

Aerial image using infrared film from an altitude of 610 m. Dark colors indicate the healthiest soybean crop, and light colors indicate less healthy crop.

Percentage reflectance of sunlight from soybean canopies in the near infrared region (810 nm) from a height of 2.7 m above the soil surface. Dark colors indicate the healthiest soybean canopy, and the lighter colors indicate a less healthy canopy.

Yield map generated using GIS software. The darkest blue colors indicate the highest yields; the darkest red colors indicate the lowest yields.

Map of Soybean Cyst Nematode population density. The darkest red color indicates the highest SCN population density.

Fig. 3.1 Overlay of GIS maps for three remote sensing platforms (satellite, aerial, and ground-based), along with maps for yield and soybean cyst nematode population density for a 1.2-ha soybean field located at Woodruff Farm, Ames, IA
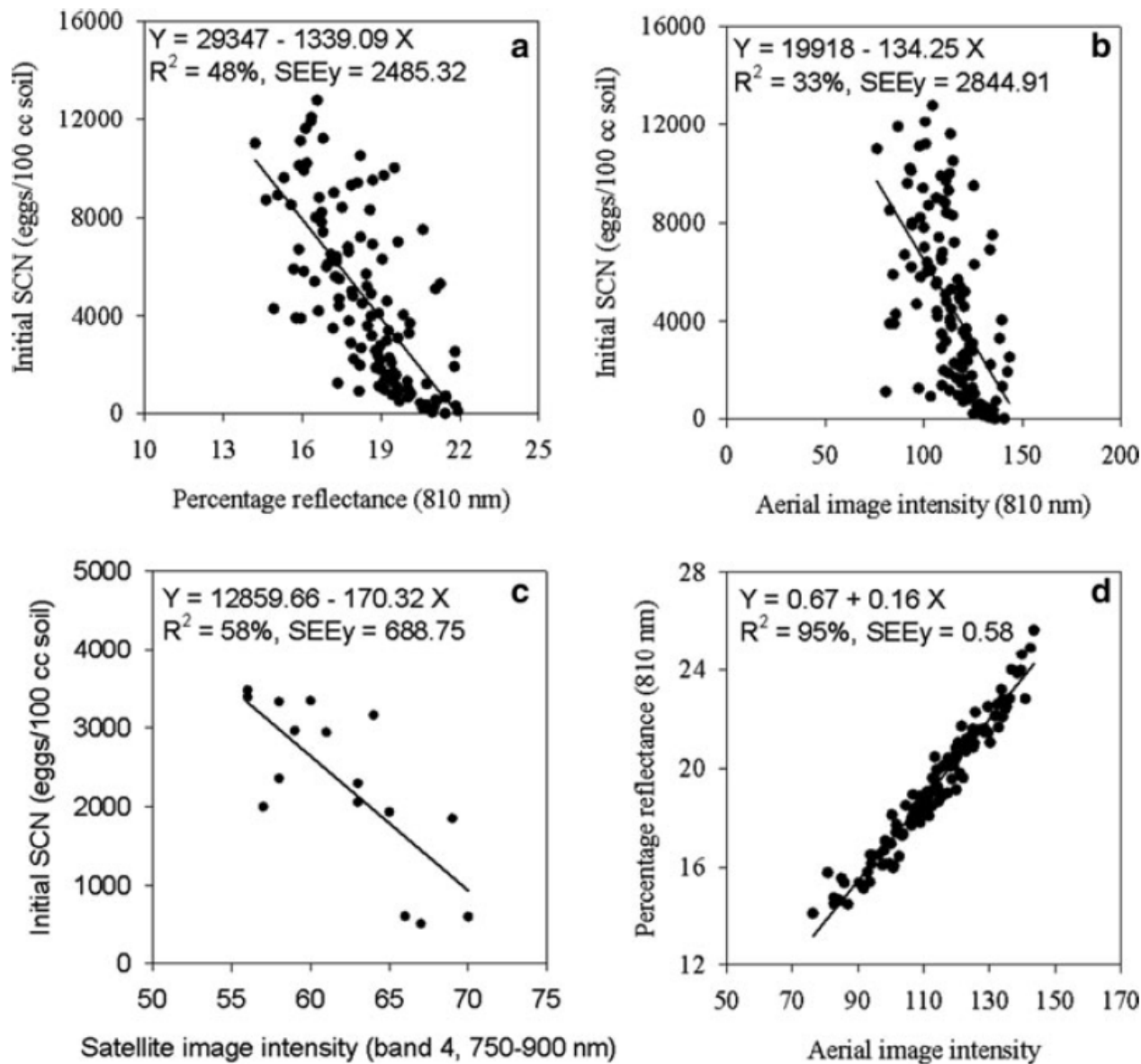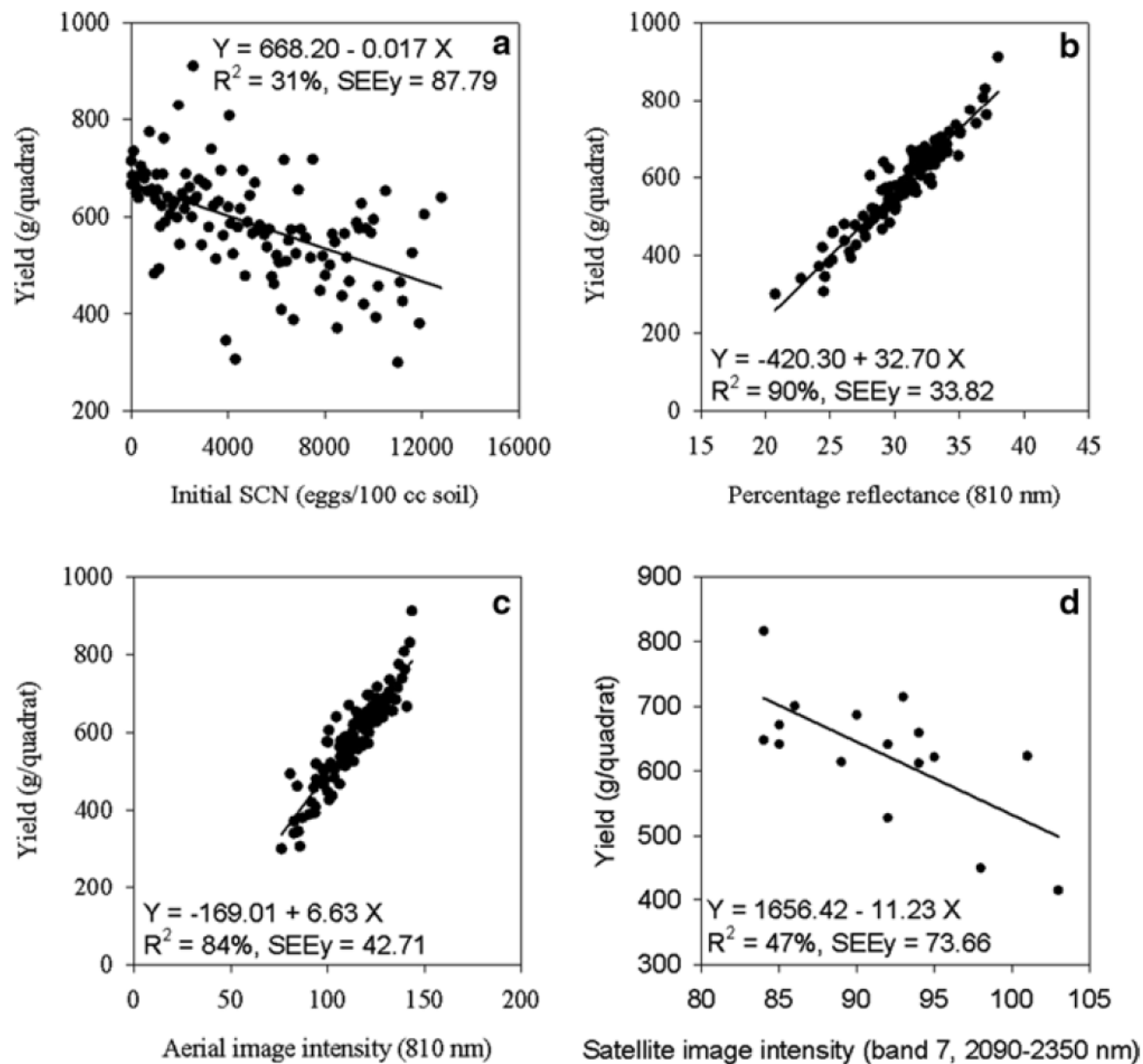
Nutter et al 2010

Fig. 3.2 Quantitative relationships between (a) ground-based, (b) aerial, and (c) satellite (Landsat 7) remote sensing data (near-infrared wavelength band) in relation to the population density of soybean cyst nematode for a soybean field located in Ames, Iowa. In (d), NIR data obtained from the aerial platform had a strong linear relationship with NIR data obtained using a ground-based multispectral radiometer (CropScan, Inc., Rochester, MN)

R^2 indica que con el uso de éstos sensores remotos se puede explicar 48%, 33% y 58% de la variación en el inóculo inicial del nemátodo formador de quistes.

Nutter et al 2010

Fig. 3.3 a–d Quantitative relationships of (**a**) SCN population density (eggs 100^{-1} ccm soil), (**b**) ground-based measurement of percentage of sunlight reflectance (810 nm), (**c**) aerial image intensity (810 nm), and (**d**) Landsat 7 satellite imagery with soybean yield, for a soybean field located in Ames, Iowa

La cantidad de inóculo inicial del nemátodo explica el 31% de la variación en Rendimiento

Los sensores remotos explican 90%, 84% y 47% de la variación en Rendimiento.

El tejido verde sano correlaciona con rendimiento pero otros factores (deficiencia de Fe por ej) afectan también la cantidad de tejido verde sano.

El satélite utilizado tiene una resolución de 4m^2

Nutter et al 2010

Supplemental figure 1. Hyperspectral imaging data cube of a barley leaf, diseased with powdery mildew, caused by *Blumeria gramins* f.sp. *hordei*. A hyperspectral data cube contains the spatial information in two dimensions and can be visualized as a pseudo-RGB image. Spectral reflectance properties for each image pixel are available from 400 to 1,000 nm and are shown as an intensity image (rainbow colors). Wavelength with maximal absorbance in the visible range and near-infrared range of different pigments and other leaf chemical compounds are indicated.
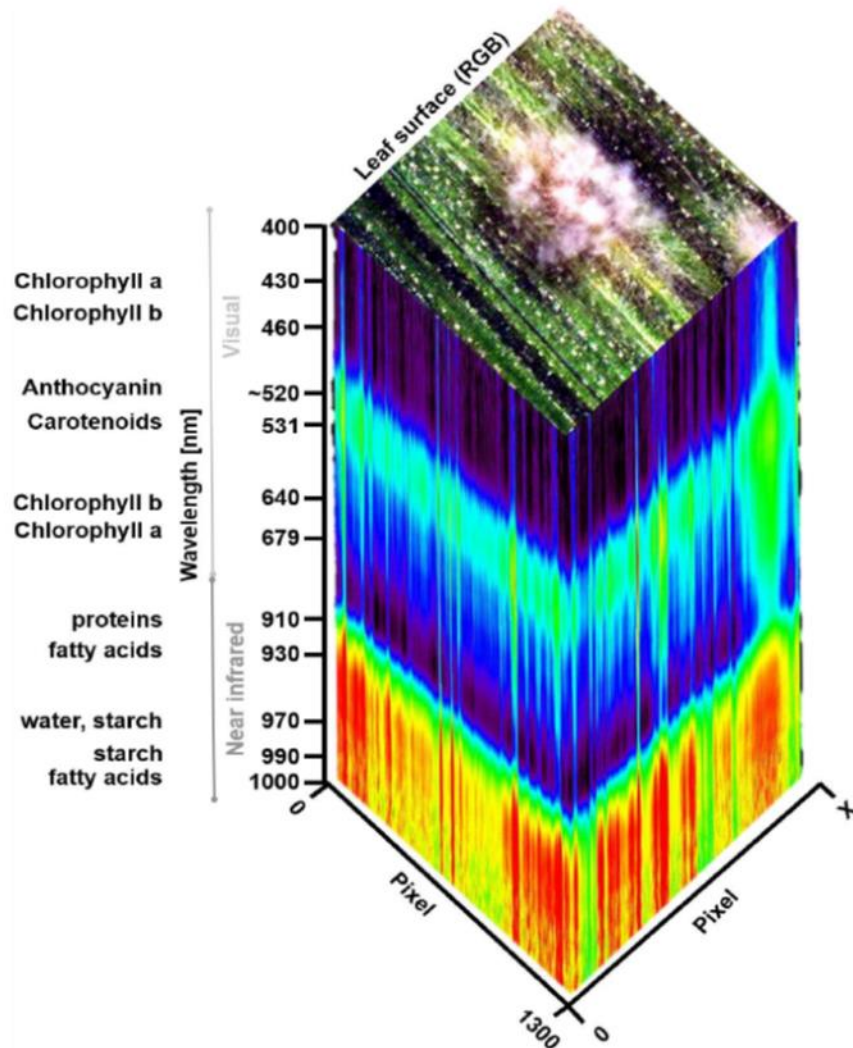
Imágenes hiper-espectrales

Este tipo de datos son matrices con eje x, eje y que definen espacio y eje z que define la reflectancia por cada longitud de onda.
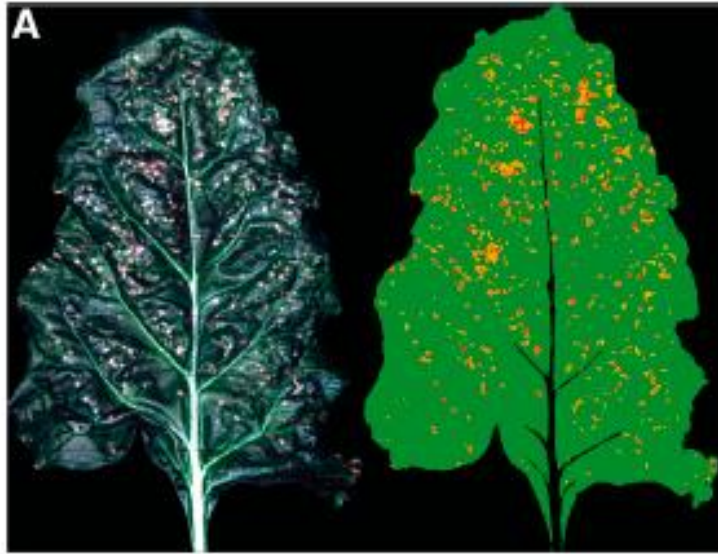
Fig. 6. Disease detection of fungal plant diseases based on hyperspectral images. A, Supervised classification (spectral angle mapper) of Cercospora leaf spot on sugar beet. The green color denotes healthy leaf tissue, the yellow color the border of Cercospora leaf spot and the red color the necrotic center of Cercospora leaf spot. B, Spikelets, diseased by Fusarium head blight, can be visualized by calculation of the normalized difference vegetation index (Photo A: A.-K. Mahlein; photo B: A.-K. Mahlein and A. Al Masri).

Imágenes hiperespectrales permiten separar tejido sano y tejido enfermo al definir un índice.

Se procesan y normalizan los datos mediante algoritmos (para compensar diferencias en iluminación por ej)

Se define un índice vegetativo: basado en la relación de las diferentes bandas se define un factor como más importante y se reducen factores de otro menor importancia.

En este ejemplo se usa NDVI (normalized difference vegetative index) para diferenciar entre tejido sano y tejido enfermo

$$NDVI = \frac{(NIR - RED)}{(NIR + RED)}$$
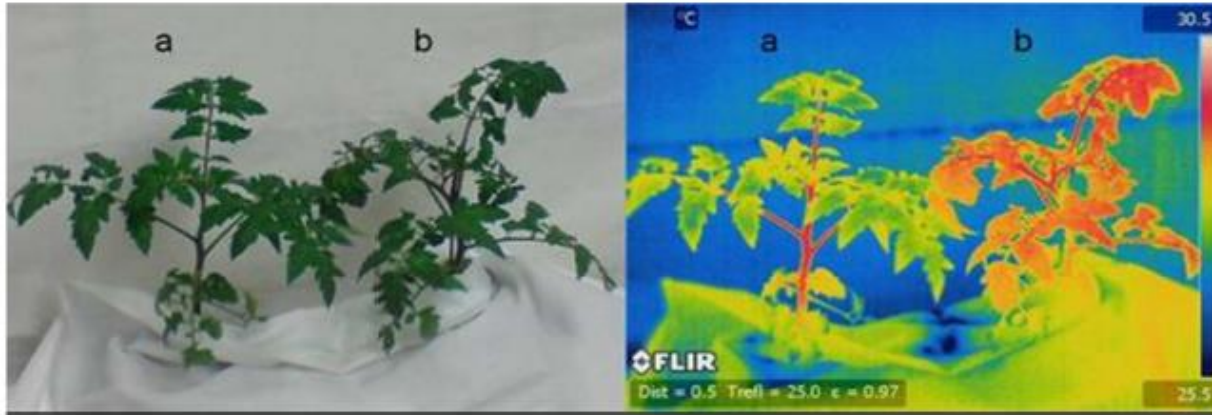
Uso de sensores térmicos

Figure 1. Digital color reflectance and thermal images of two tomato plants, healthy (a) and infected plant (b) with *R. solanacearum*, six days after inoculation.

Uso de cámara térmica permite detección temprana de la enfermedad

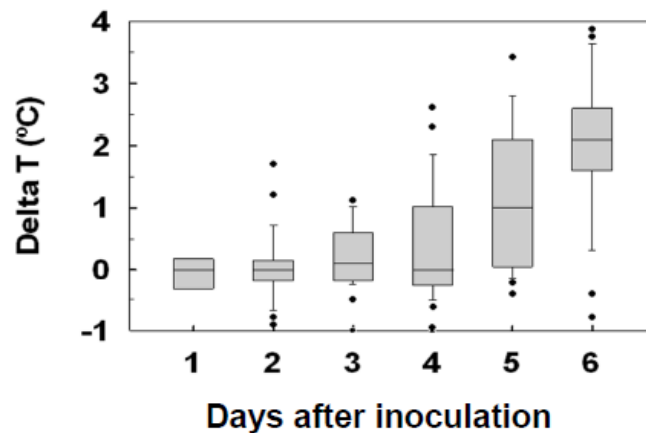Permite varias mediciones en el tiempo sobre la misma planta

Figure 2. Differences in leaf temperature of plants infected with *R. solanacearum*, six days after inoculation.
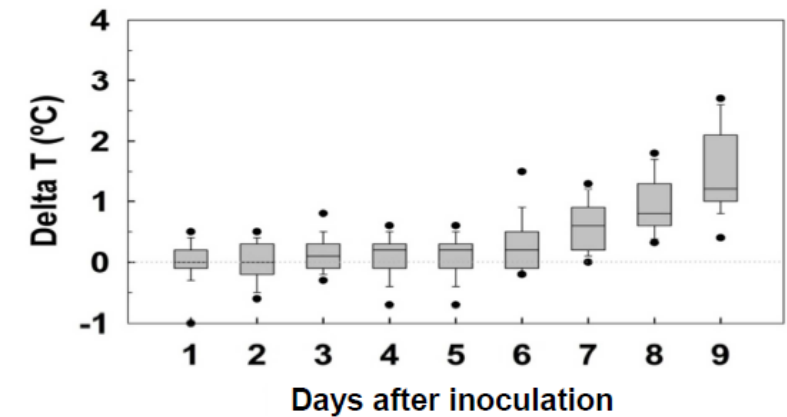

Figure 3. Differences in leaf temperature of plants infected with *R. solanacearum*, during the nine days after inoculation.

Rep1
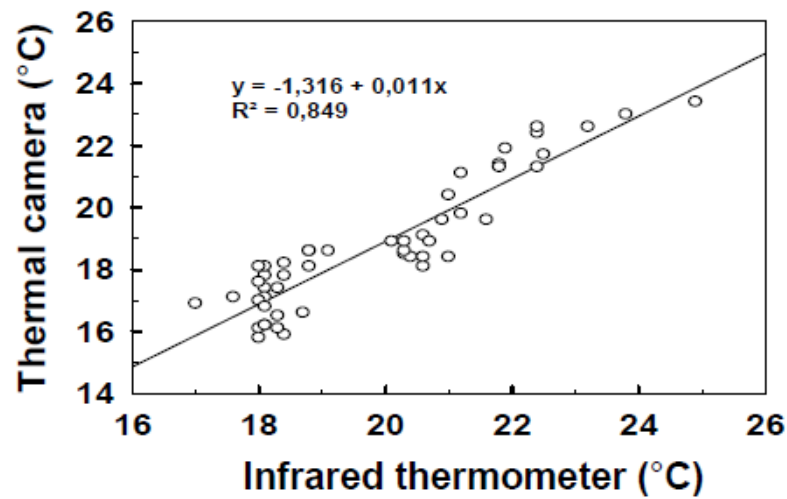
Rep2 (se realizó con condiciones más frías)

Calderón et al 2014

Figure 4. Correlation between leaf temperature measured thermographically and using the infrared thermometer.

$y = -1,316 + 0,011x$
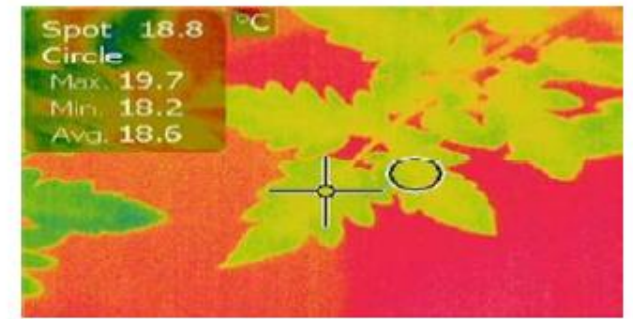$R^2 = 0,849$

Figura 13. Capacidad de la cámara infrarroja de medir la temperatura de un área específica, en este caso un punto y un círculo de 1 cm de diámetro.

Figura 10. Área de evaluación de dos plantas en un sistema pareado, una de ellas está inoculada, mientras que la otra está sana.

Figura 12. Manera de medir la temperatura con el termómetro infrarrojo.

Calderón 2013
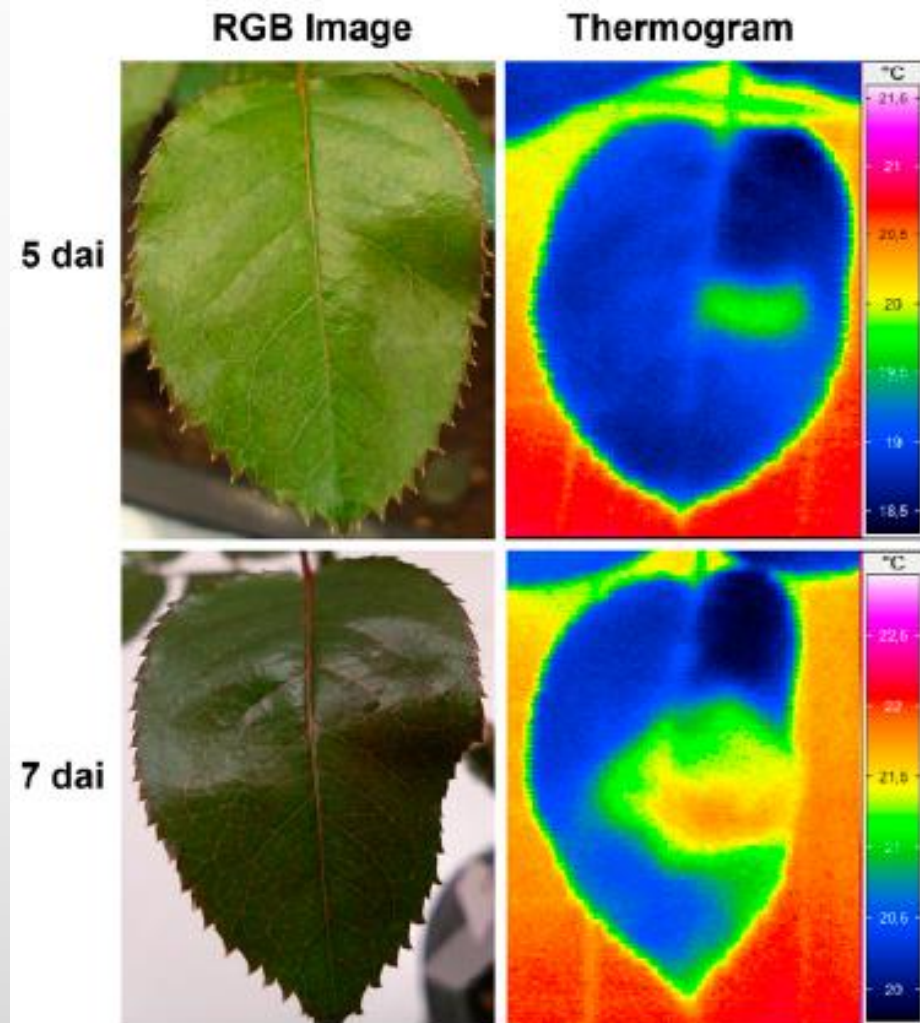
RGB Image   **Thermogram**

5 dai

7 dai

Fig. 7. Monitoring of rose leaf colonization by *Peronospora sparsa* and symptom development of downy mildew in early stages (5 and 7 days after inoculation) of the disease by thermographic imaging. (Photo: S. Gomez).

Detección temprana de mildiú velloso en rosa.

Malheim 2015

Sensors

RGB   Multispectral   Hyperspectral   Thermal   Chlorophyll-Fluorescence   3D-Sensors

Biomass Vitality

Diseased Aereas

Disease Symptoms

Defence Reactions

Plant Phenotyping
Resistance Breeding
Pathogenicity Tests
Fungicide Screening

High Throuput Platforms
Microscope
Vehicle based
UAV
Airplane
Satellite

Precision Crop Protection
Decision Making
Site Specific Application

Cell   Leaf   Plant   Plot   Field   Ecosystem

Experimental Protocol

GIS / GPS

Soil / Site Variability
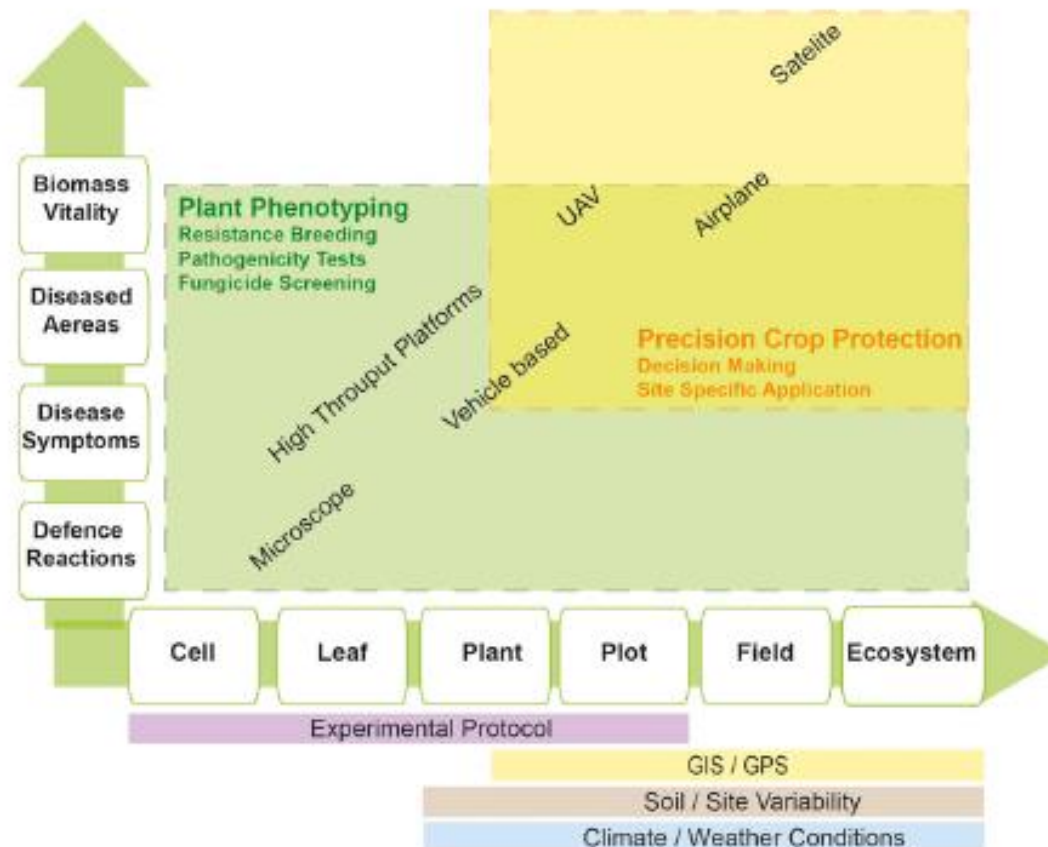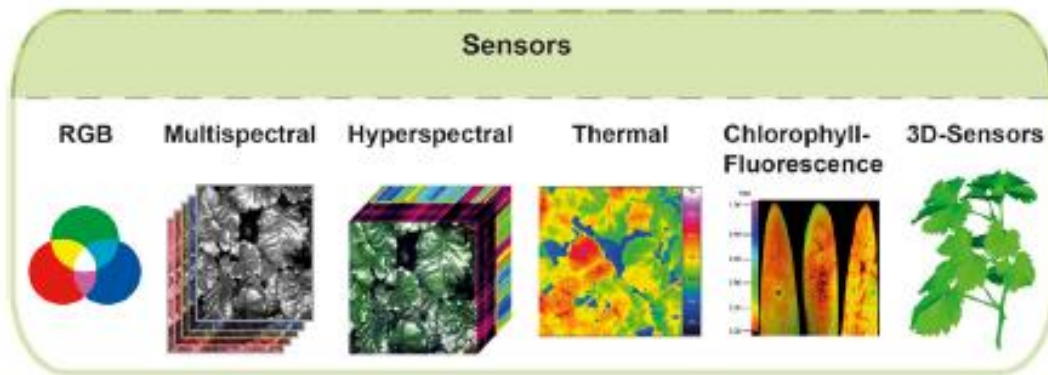
Climate / Weather Conditions

Fig. 2. Overview of current sensor technologies used for the automated detection and identification of host-plant interactions. These sensors can be implemented in precision agriculture applications and plant phenotyping on different scales from single cells to entire ecosystems. Depending on the scale, different platforms can be operated and consequentially different plant parameters can be observed (Oerke et al. 2014, modified).

Fig. 5 Cost and availability of imaging spectroscopy data could be improved using an Unmanned Aerial Vehicle (UAV) remote sensing system. The md4-1000 UAV used by Torres-Sánchez et al. (2013) can carry any sensor weighing less than 1.25 kg. For evaluation of weed infestation, it was equipped with a still point-and-shoot camera and a six-band multispectral camera (courtesy of Public Library of Science)

Hyperspectral microscope images

Automated monitoring disease progress
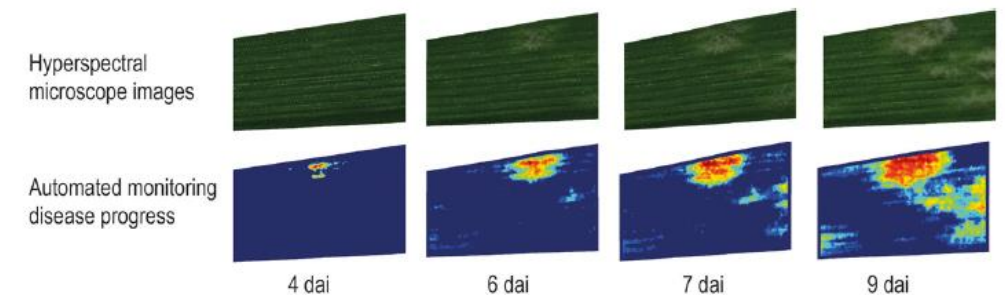
4 dai   6 dai   7 dai   9 dai

Fig. 8. Powdery mildew progress on a susceptible barley genotype cv. Ingrid assessed by a hyperspectral microscope (Kuska et al. 2015). Using this small-scale approach, the phenotyping and differentiation of different genotypes is possible. (Photo: A.-K. Mahlein, M. Kuska, and M. Wahabzada).

Malheim 2015

Limitaciones y retos futuros en el uso de sensores remotos

- Aunque resulta de utilidad para la cuantificación de enfermedades, para un mayor aprovechamiento se requiere mayor desarrollo en el área de detección temprana de enfermedades.

- La detección específica de una enfermedad se complica en condiciones de campo cuando varios tipos de estrés están presentes en la planta.
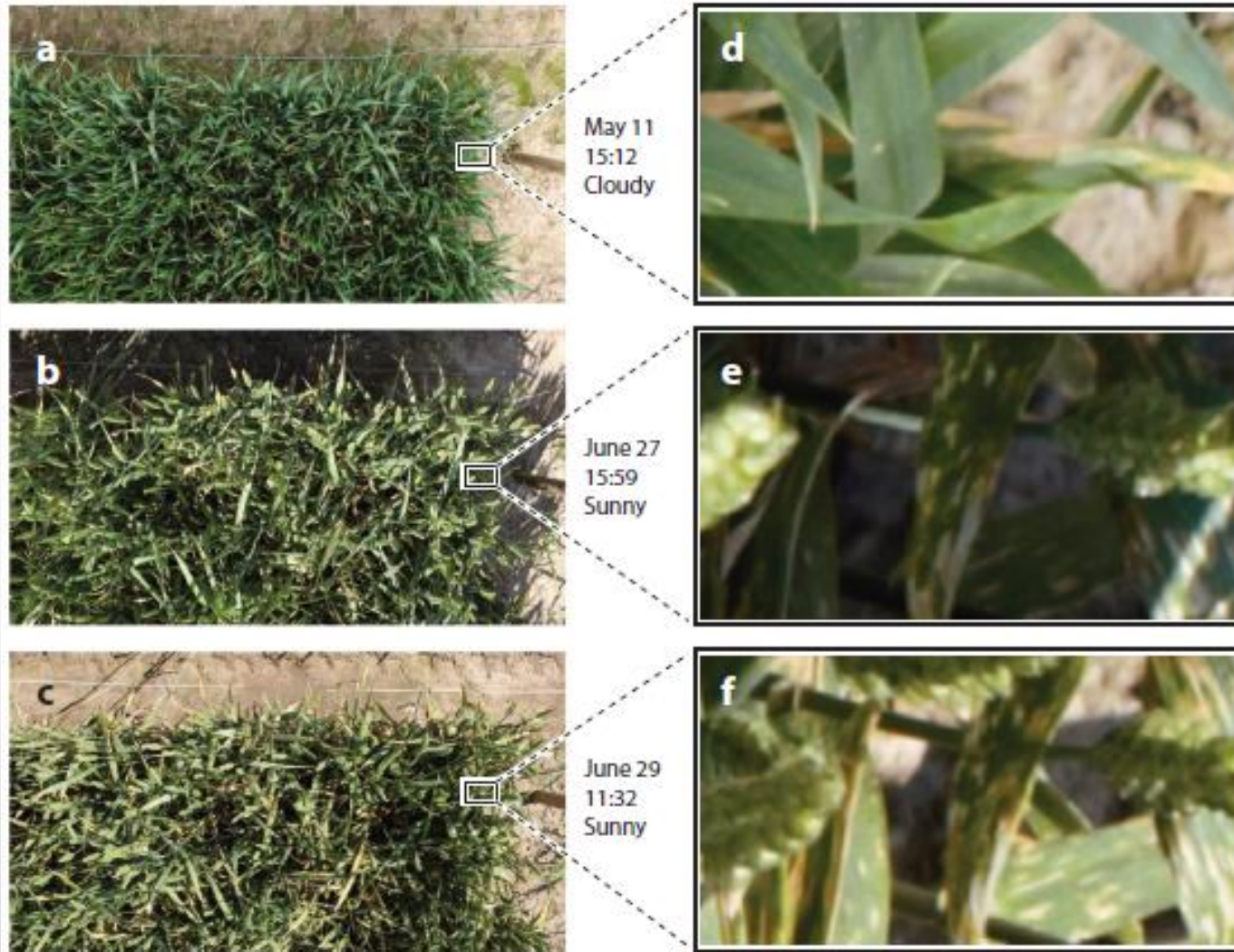
Figure 3

Wheat canopy affected by Septoria leaf blotch during later stages of development. Images were taken with the digital single lens reflex camera of the field phenotyping platform of ETH Zürich (80) from a distance of 3 m on three different days of the year 2016. Panels *a*, *b*, and *c* show sections of ca. 100 × 50 cm; panels *d*, *e*, and *f* show magnified subsections of panels *a*, *b*, and *c*, respectively.

- La mayoría de experimentos se ha realizado bajo condiciones controladas en donde se usa iluminación artificial.

- En condiciones de campo la luminosidad es variable, la luz puede tener diferentes ángulos, y luminosidad puede también variar en diferentes lugares de la plantación simultáneamente.

- En ocasiones se requiere distinguir entre tejido enfermo y tejido senescente

- La estructura del dosel produce cambios en la forma que se refleja la luz recibida.
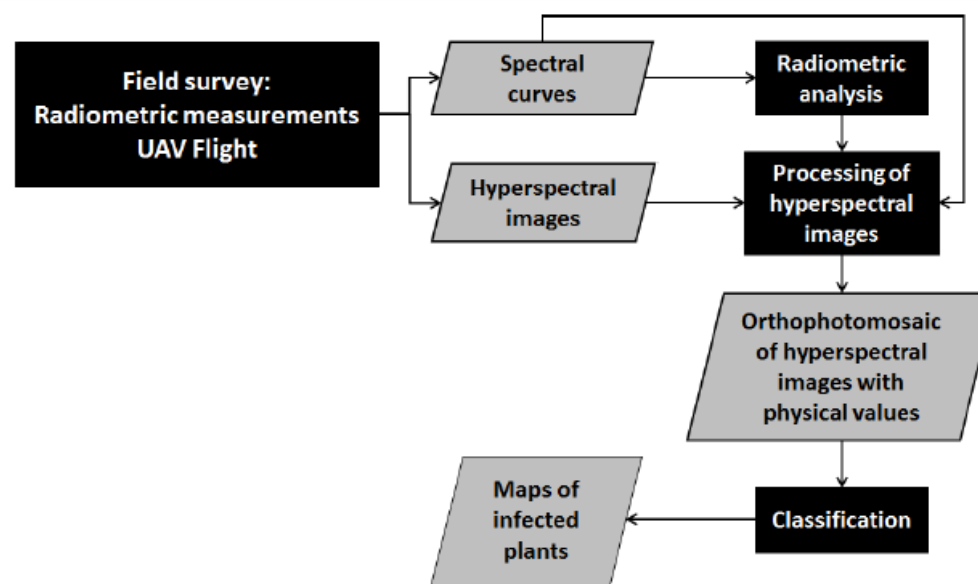
Figure 3. (a) Healthy orange. (b) Orange with HLB.
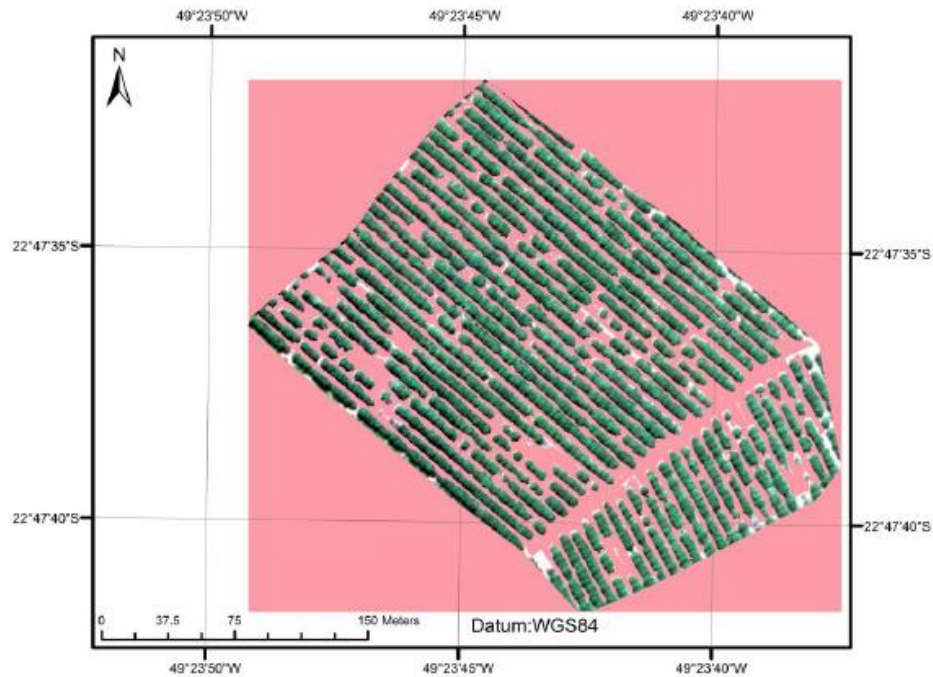

Figure 4. Flowchart of hyperspectral cube processing

Figure 5. Orthophotomosaic radiometrically corrected.

Legend
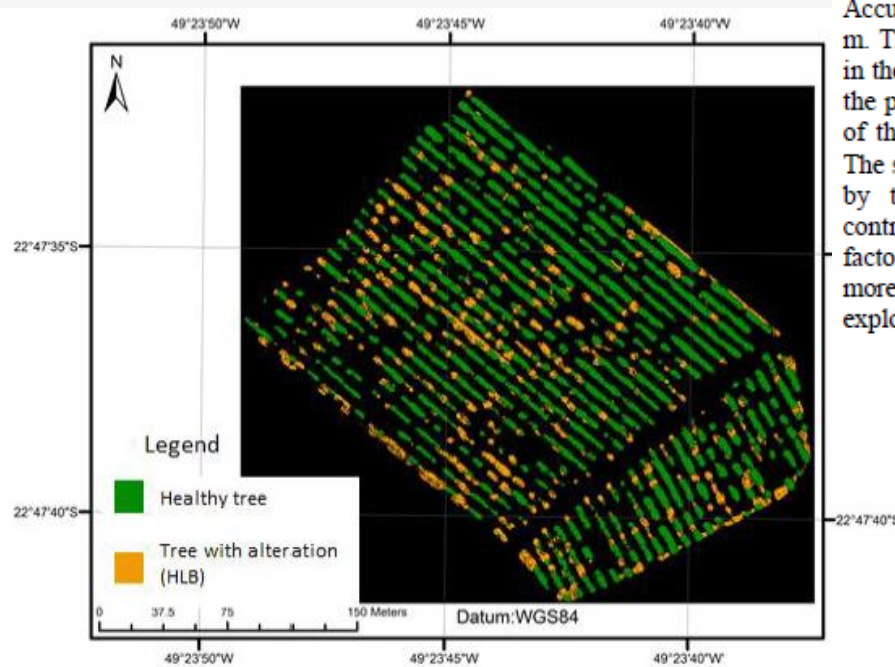- Healthy tree
- Tree with alteration (HLB)

Figure 7. Citrus health map.

Accuracy in the detection of HLB was 61.2% for GSD of 0.50 m. The high detection of false positives is a challenging factor in the differentiation of plants with HLB. The hypothesis is that the presence of weeds at the edge of the tree caused confusion of the classifier in differentiating the plants infected by HLB. The saturation of the image and the presence of shadows caused by the citrus canopy architecture itself, are factors that contributed to the high number of false positives. All these factors should be better evaluated and more thoroughly and more efficient automatic processing solutions should be explored.

Moriya et al 2019